

## Zone-folding effect in short-period $(\text{GaAs})_n/(\text{AlAs})_n$ superlattices with $n$ in the range 3–15

T. Matsuoka, T. Nakazawa, T. Ohya, K. Taniguchi, and C. Hamaguchi

*Department of Electronic Engineering, Faculty of Engineering, Osaka University, Suita City, Osaka 565, Japan*

H. Kato and Y. Watanabe

*Department of Physics, School of Science, Kansai Gakuin University, Nishinomiya City, Hyogo 662, Japan*

(Received 26 November 1990)

Photoreflectance and photoluminescence measurements are carried out in the temperature range from 25 to 275 K to clarify the optical properties of  $(\text{GaAs})_n/(\text{AlAs})_n$  ( $n = 3\text{--}15$ ) short-period superlattices. Our primary interest is in the zone-folded weak transition. Weak signals of photoreflectance associated with the critical point of the pseudodirect transition, a weakly allowed direct transition arising from the zone-folding effect, have been found below the main signals associated with the direct allowed transitions for  $(\text{GaAs})_n/(\text{AlAs})_n$  superlattices with  $n < 12$  at 200 K. Photoluminescence peaks appear at photon energies corresponding to the critical points of this weak structure. This assignment is supported by the temperature dependence of the photoluminescence intensity, which gives the transition probability ratio of the allowed direct-to-pseudodirect transition of about  $10^4$ . Energy-band calculations are performed by using the empirical  $sp^3$  tight-binding method including second-nearest-neighbor interactions, where the tight-binding parameters are determined to fit the effective masses of the conduction band at the  $X$  point. These calculations show the existence of a weakly allowed direct transition below the strongly allowed direct transition edge in  $(\text{GaAs})_n/(\text{AlAs})_n$  superlattices with  $n < 12$ , which shows a good agreement with the present experimental results. These results strongly suggest that the observed weak structures in the photoreflectance arise from the pseudodirect transition, indicating that the conduction band reflects the nature of the zone-folding effect ( $X_z$ -like state at the  $\Gamma$  point).

### I. INTRODUCTION

The development of crystal-growth techniques, such as molecular-beam epitaxy (MBE), has made it possible to produce superlattices (SL's) of high quality. The optical properties of GaAs/AlAs short-period SL's differ greatly from those of the alloy  $\text{Al}_x\text{Ga}_{1-x}\text{As}$  of equivalent mean composition, showing the importance of the superlattice periodicity in determining the electronic properties of these structures. Some experimental investigations have shown whether the lowest-energy transition is direct, indirect, or so-called pseudodirect and how it changes as the layer thickness is decreased.<sup>1–7</sup> From a theoretical point of view, the energy-band structure of the SL's has been investigated by the tight-binding method,<sup>8–15</sup> the Wannier-function method,<sup>16,17</sup> the pseudopotential method,<sup>18–21</sup> and the first-principles self-consistent local density approximation (LDA).<sup>22–26</sup>

In SL's where the coupling through penetrable barriers plays an important role, a miniband is formed because of delocalization of the wave function. Electrons at the states at the  $\Gamma$  point of the Brillouin zone of  $(\text{GaAs})_n/(\text{AlAs})_n$  SL's tend to be confined in either GaAs ( $\Gamma$ -like state) or AlAs ( $X_z$ -like state) layers.<sup>12</sup> The  $\Gamma$ -like conduction state is associated with the  $\Gamma$  conduction-band edge of GaAs, while the  $X_z$ -like state is associated with

the  $X$  conduction-band edge of AlAs because the  $X$  conduction valleys of AlAs lie lower than those of GaAs due to valence-band offset. Only the  $X_z$  minima are mapped onto the  $\Gamma$  point of the Brillouin zone of the SL's due to the zone-folding effect, while the  $X_{xy}$  minima are at the  $M$  point of the Brillouin zone of the SL's ( $X_{xy}$ -like state). Since holes at the  $\Gamma$  maximum of the Brillouin zone of the SL's tend to be confined in GaAs layers, the transition associated with the  $\Gamma$ -like conduction state has large transition probability, while that associated with the  $X_z$ -like state has small transition probability. Therefore, the  $\Gamma$ -like,  $X_{xy}$ -like, and  $X_z$ -like states give the direct, indirect, and pseudodirect (weakly allowed direct) transitions, respectively.

In our previous work, we reported photoreflectance (PR) and photoluminescence (PL) measurements at room temperature in  $(\text{GaAs})_m/(\text{AlAs})_5$  ( $m = 3\text{--}11$ ) (Ref. 27) and  $(\text{GaAs})_n/(\text{AlAs})_n$  ( $n = 1\text{--}15$ ) SL's.<sup>28</sup> The experimental results of the former SL's show that the band crossing occurs at  $m = 7$ , while the latter occurs at  $n = 10$ . This conclusion was drawn from the fact that the observed photoluminescence peaks at the lower-energy side lie well below the transition energies obtained from PR data and that the transition energy of PR reflects a direct band gap, whereas the lowest-energy PL peak reflects lower-energy band gap (direct, pseudodi-

rect, or indirect). Our theoretical calculations based on the  $sp^3s^*$  tight-binding method<sup>12,29</sup> support the experimental observations, where the crossover of the direct and indirect transitions occurs at  $m = 7$  for  $(\text{GaAs})_m/(\text{AlAs})_5$  SL's and at  $n = 8$  for  $(\text{GaAs})_n/(\text{AlAs})_n$  SL's. The tight-binding calculations by Ihm demonstrated that if the GaAs layer thickness is less than about 30 Å, the lowest conduction state is the  $X_{xy}$ -like state resulting in the indirect transition.<sup>15</sup> The effective-mass approximation, however, indicates an existence of a crossover of the  $X_z$ -like and  $\Gamma$ -like states.<sup>4,5,7</sup> This controversy is ascribed to the difference in the effective masses at the  $X$ -point valley. It is shown that the tight-binding calculations based on the nearest-neighbor interaction give an infinite transverse effective mass in the  $X$  valley of the bulk bands.<sup>30,31</sup> The tight-binding calculations made by Yamaguchi<sup>12</sup> and the present authors<sup>28</sup> take into account the second-nearest-neighbor interaction in order to fit the energy at the  $L$  point of the bulk bands, but the dispersion at the  $X$  point is similar to the results of nearest-neighbor calculations. Recently using the second-nearest-neighbor  $sp^3$  tight-binding method by Lu and Sham,<sup>30</sup> this controversy has been resolved and assignments by this tight-binding method coincide with those of the effective-mass approximation. In this tight-binding calculation, the anisotropy of the effective masses of AlAs at the  $X$  point ( $m_l = 1.1m_0$ ,  $m_t = 0.19m_0$ ) is considered and it is demonstrated that  $X_z$ -like conduction states lie below  $X_{xy}$ -like conduction states. Xia and Chang<sup>31</sup> also have investigated the band structures of GaAs/AlAs SL's using this method, and obtained results similar to those of Lu and Sham.<sup>30</sup>

In our previous paper<sup>28</sup> we observed a weak structure below the strong structure in  $(\text{GaAs})_5/(\text{AlAs})_5$  SL at room temperature, where the transition energy of the weak structure corresponds to the PL peak at the low-energy side. We pointed out that this result may be interpreted in terms of the weak structure arising from the zone-folding effect, that is, the transition between the zone-folded  $X_z$ -like conduction band and the valence-band top at the  $\Gamma$  point. Since this weak structure on PR was observed only in  $(\text{GaAs})_5/(\text{AlAs})_5$  SL, we were not able to confirm the existence of the pseudodirect transition. In our recent study,<sup>32,33</sup> where we very carefully carried out similar experiments by changing the temperature and improving the sensitivity of the detection, we observed the weak structure in  $(\text{GaAs})_n/(\text{AlAs})_n$  SL's with  $n$  less than about 12. Therefore, we concluded that the weak structure in PR arises from the pseudodirect (weakly allowed direct) transition.

In this paper we will report PR and PL measurements in the  $(\text{GaAs})_n/(\text{AlAs})_n$  SL's in the temperature range from 25 to 275 K, where the SL's are grown very carefully in the range  $n$  from 3 to 15. We compare the experimental results with the energy-band calculations based on the second-nearest-neighbor  $sp^3$  tight-binding method,<sup>30,31</sup> since this method is better than the previous calculations based on the  $sp^3s^*$  tight-binding method. In Sec. II we describe experimental procedures. In Sec. III we present

results of PR measurements and compare with PL data. We also present theoretical calculations of energy-band structure using the second-nearest-neighbor  $sp^3$  tight-binding method in Sec. III, where we discuss the pseudodirect transition, and then compare the results with the experimental data. Finally we summarize the present results.

## II. EXPERIMENTAL PROCEDURES

The set of  $(\text{GaAs})_n/(\text{AlAs})_n$  samples used in this work were epitaxially grown at 570 °C on (100) semi-insulating GaAs substrates by MBE. The values of atomic layer number  $n$  were 3–15 and the multiple layers were about 200 periods. The number of GaAs and AlAs layers was accurately controlled by counting the period of the intensity oscillations of a specularly reflected beam in a reflection high-energy electron diffraction (RHEED) pattern.<sup>34</sup> The thickness of the individual atomic layer of the SL's has been measured using the x-ray diffraction method.<sup>35</sup>

The experimental arrangement of PR measurements used in the present work is reported elsewhere,<sup>27,28,36</sup> and is basically similar to that used by Shay<sup>37</sup> and Glembocki *et al.*<sup>38</sup> The modulation is accomplished by mechanically chopping a laser of photon energy greater than the band gap of the sample. In the present work we used an Ar-ion laser chopped at a frequency of 210 Hz. The intensity of the Ar-ion laser, 488.0 or 476.5 nm, was about 0.2 mW.

## III. RESULTS AND DISCUSSION

Figure 1 shows PR (open circles) and PL (dot-dashed curve) experimental spectra at 200 K together with the analytical PR spectra best fitted to the PR data (solid curve) for (a)  $(\text{GaAs})_8/(\text{AlAs})_8$  and (b)  $(\text{GaAs})_{12}/(\text{AlAs})_{12}$  SL's, where the vertical arrow indicates the critical point energies obtained by the fitting procedure. Representative values of PR data are plotted. The experimental data of PR are analyzed using the third-derivative formula derived by Aspnes,<sup>39,40</sup> which is given by

$$\frac{\Delta R}{R} = \sum_j^p \text{Re}[C_j \exp(i\theta_j)(E - E_{g_j} + i\Gamma_j)^{-m_j}], \quad (1)$$

where  $p$  is the number of critical points,  $E$  the photon energy,  $C_j$ ,  $\theta_j$ ,  $E_{g_j}$ , and  $\Gamma_j$  are the amplitude, phase, energy gap, and broadening parameter, respectively, of the  $j$ th critical point. The value of  $m_j$  is a parameter which depends on the critical point type,  $m_j = 4 - D/2$  for the  $D$ -dimensional critical point. As the electrons and holes are extended in the SL's, the critical points are expected to be three dimensional and we use  $m_j = 2.5$ . The values of the parameters stated above are evaluated by fitting the line shape of the third-derivative formula to the experimental data of PR, based on the method proposed

by Rosenbrock.<sup>41</sup> Details of the reflectance analysis are given elsewhere.<sup>27,28,32,36</sup>

In Fig. 1(a) we find that the PL spectrum consists of two main peaks, while the PR spectrum exhibits a weak structure at a lower-energy side and a very complicated structure, where the latter structure seems to reflect an existence of many critical points in the energy range 1.85–2.0 eV. The lower-energy structure around 1.8 eV (the estimated critical point energy is 1.797 eV) is very weak compared to the structures at 1.897, 1.915, and 1.951 eV. The PL peaks at 1.815 and 1.902 eV seem to correspond to the PR structures at 1.8 and 1.9 eV. The lower-energy weak PR structure in Fig. 1(a) is assigned to a direct transition at the  $\Gamma$  point associated with the zone-folded ( $X_2$ -like) conduction band. This is because the PR spectra arise from the critical points of the joint density of

states and thus from the direct transition process. Therefore, these weak structures in the PR spectra originate from the weakly allowed direct (pseudodirect) transition between the zone-folded conduction band ( $X_2$ -like state) and the valence-band top. The higher-energy transitions at 1.897, 1.915, and 1.951 eV of the PR spectra are interpreted in terms of the allowed direct transitions at the  $\Gamma$  point.

Figure 1(b) represents PL and PR spectra for  $(\text{GaAs})_{12}/(\text{AlAs})_{12}$  SL at 200 K, where we find a main peak and a weak shoulder at the higher-energy side in the PL spectrum. The PR spectra in Fig. 1(b) show that the weak structure in the lower-energy region merges into the main structure and thus three transitions exist in a narrow photon energy region from 1.7 to 1.85 eV. These results shown in Figs. 1(a) and 1(b) demonstrate the higher resolution of PR measurements compared to PL measurements. The weak shoulder of the PL spectra may be resolved at lower temperatures.

In order to support the above assignment, we investigated the temperature dependence of PL intensities. As shown below, crossover of the intensity ratio of the two PL peaks associated with the weak and strong PR structures is expected when the recombination rate of the former structure is weaker than that of the latter. The temperature dependence of the PL spectra for  $(\text{GaAs})_7/(\text{AlAs})_7$  SL is shown in Fig. 2, where the intensity of the PL peak at the higher-energy side decreases and the other peak at the lower-energy side increases as the tempera-

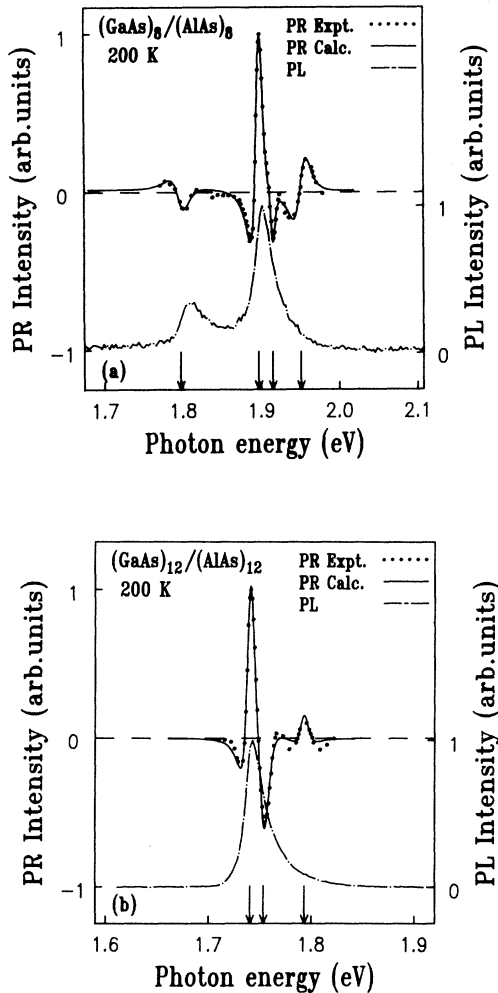


FIG. 1. PR (open circles) and PL (dot-dashed curve) spectra at 200 K for (a)  $(\text{GaAs})_8/(\text{AlAs})_8$  and (b)  $(\text{GaAs})_{12}/(\text{AlAs})_{12}$  SL samples. The solid curve is determined by fitting the line shape of Eq. (1) to the PR experimental spectrum. Representative values of PR data are plotted. The vertical arrows indicate the interband transition energies obtained by the fitting procedure.

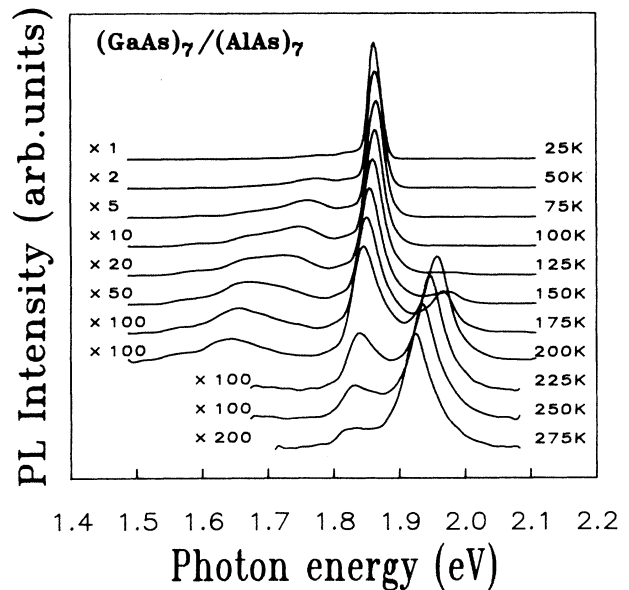


FIG. 2. PL spectra of  $(\text{GaAs})_7/(\text{AlAs})_7$  SL are plotted at various temperatures (from 25 to 275 K). Lower- and higher-energy peaks are assigned to be the pseudodirect and allowed direct transitions, respectively. The temperature dependence of the PL intensities are interpreted in terms of the difference in the transition probabilities and the change in the electron population in the  $\Gamma$ -like and  $X_2$ -like conduction bands (see text in detail).

ture decreases. Based on the discussion stated above, the higher- and lower-energy peaks are assigned to the direct and pseudodirect transitions, respectively. The intensity of emission depends on the transition probability and the number of carriers excited. In the following, we neglect the effect of reabsorption. With this approximation, we are able to estimate the transition probability. Under this assumption the PL intensity is proportional to the product of electron density at the conduction band and the transition probability, and the ratio of PL emission between the direct and the pseudodirect band gap is therefore written as

$$\frac{I(\Gamma)}{I(X)} = \left(\frac{m_\Gamma}{m_X}\right)^{3/2} \frac{W_\Gamma}{W_X} \exp\left(\frac{E_X - E_\Gamma}{k_B T}\right), \quad (2)$$

where  $I(\Gamma)$ ,  $E_\Gamma$ , and  $W_\Gamma$  are the PL intensity, transition energy, and transition probability for the direct allowed transition, and  $I(X)$ ,  $E_X$ , and  $W_X$  for the pseudodirect transition,  $m_\Gamma$  and  $m_X$  are the density-of-states masses in  $\Gamma$ -like and  $X_z$ -like conduction bands, and  $k_B$  is the Boltzmann constant. The factor  $(m_\Gamma/m_X)^{3/2}$  is the ratio of the density of states in the  $\Gamma$ -like and  $X_z$ -like conduction bands.

Figure 3 shows the intensity ratio  $I(\Gamma)/I(X)$  as a function of inverse temperature with the least-square-fit lines for  $(\text{GaAs})_n/(\text{AlAs})_n$  SL's with  $n = 5, 7, 8, 10$ , and  $12$ . The energy separation  $E_\Gamma - E_X$  obtained from the slope of the line is in reasonable agreement with the PL peak energy separation [within 10% difference except for the  $(\text{GaAs})_{12}/(\text{AlAs})_{12}$  SL]. From the intercept of the line the ratio of the transition probabilities  $W_X/W_\Gamma$  is estimated to be  $6.7 \times 10^{-4}$ ,  $1.6 \times 10^{-4}$ ,  $2.5 \times 10^{-4}$ ,  $2.7 \times 10^{-4}$ , and  $8.3 \times 10^{-4}$  for  $n = 5, 7, 8, 10$ , and  $12$ , respectively. Here,

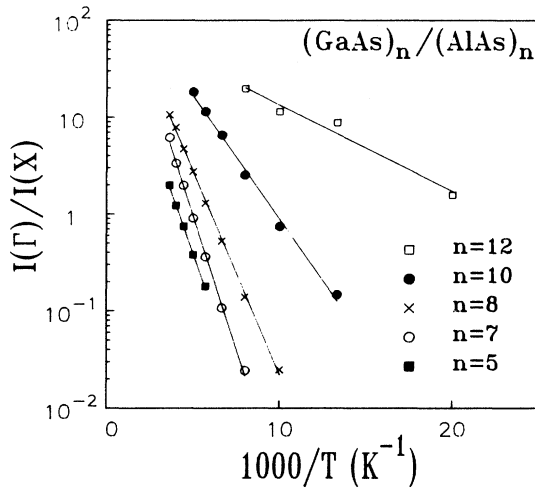


FIG. 3. The ratio of the PL peak intensity of the allowed direct transition to the pseudodirect transition is plotted as a function of inverse temperature for the  $(\text{GaAs})_n/(\text{AlAs})_n$  SL's with  $n = 5, 7, 8, 10$ , and  $12$ , where the slope gives the energy separation and the intercept of the line at zero gives the ratio of the transition probabilities (see text in detail).

the values of  $m_\Gamma$  and  $m_X$  are assumed to be equal to the density-of-states mass of GaAs and AlAs bulks, respectively ( $m_\Gamma = 0.068m_0$  and  $m_X = 0.34m_0$ ). The ratio of the transition probability suggests that the transition at the lower-energy side is much weaker (by 3 or 4 orders of magnitude). Therefore, these results strongly suggest that the lower-energy weak transition is ascribed to a pseudodirect band gap at the  $\Gamma$  point associated with the  $X_z$ -like state, resulting from the zone folding.

It is very interesting to investigate the temperature dependence of the transition energies in  $(\text{GaAs})_n/(\text{AlAs})_n$  SL's. Figure 4 shows the temperature dependence of the transition energies in  $(\text{GaAs})_8/(\text{AlAs})_8$  SL, where transition energies determined from the PR and PL measurements are plotted by the circles (open circles for the strong structures and solid circles for the weak structures) and crosses, respectively. We find in Fig. 4 that the three transition energies of the strong structures in the PR spectra decrease monotonically with increasing temperature and the shift is about 100 meV in the temperature range from 25 to 275 K. The higher-energy peak of the PL spectra shows a very similar temperature dependence to the lowest critical point energy of the strong PR structures. The critical point energy of the weak structure in the PR spectra which is ascribed to the pseudodirect transition exhibits a temperature dependence similar to the higher critical point energies, while the PL peak at the lower-energy side shows a weaker temperature dependence compared to the others (about 70 meV shift in the same temperature range). The difference in the transition energies between the weak structure of the PR spectra and the lowest PL peak increases with increasing temperature and becomes about 20–30 meV at higher temperatures. The difference exceeds the range of

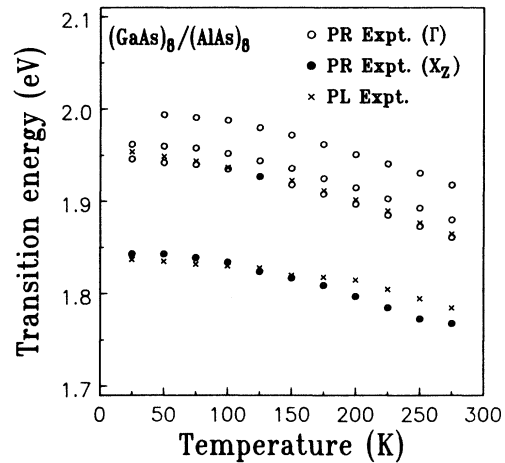


FIG. 4. The transition energies obtained by PR and PL measurements in the  $(\text{GaAs})_8/(\text{AlAs})_8$  SL are plotted as a function of temperature, where the open (higher transition energies, allowed direct) and solid (lower transition energies, pseudodirect) circles are the energies determined from the PR measurements, and the crosses are PL peak energies.

experimental error and is not clear at the present stage. The energy shift of the transition energies determined from the PR experiments is quite similar to that of the fundamental energy gap of GaAs bulk. Noting that the pseudodirect gap reflects the nature of the conduction band at the  $X$  point of AlAs, its temperature dependence is expected to be weaker compared to that of the allowed direct band gap. In Fig. 4 we found that the pseudodirect gap obtained from the PR experiments behaves quite similarly to that of the direct gap of GaAs, although the gap determined from the PL data behaves similarly to that of indirect band gap of AlAs. Similar behavior is observed in other  $(\text{GaAs})_n/(\text{AlAs})_n$  SL's.

In Fig. 5 we plot the transition energy corresponding to the main structure of the PR signals (the lowest allowed direct transition energy) as a function of temperature for  $(\text{GaAs})_n/(\text{AlAs})_n$  SL's with  $n = 3-15$ . All the samples exhibit a quite similar feature in their temperature dependence. Taking into account the fact that the conduction band associated with this transition reflects the nature of the conduction band of GaAs at the  $\Gamma$  point, its temperature dependence is expected to be similar to that of GaAs. The temperature dependence of the transition energies may be calculated by using the tight-binding theory when we take into account the temperature dependence of the bond lengths and bond angles. We have not yet performed such calculations.

In Figs. 6(a), 6(b), and 6(c) we show the monolayer number  $n$  dependence of the transition energies determined from the PR and PL measurements at 250, 150, and 50 K, respectively, in  $(\text{GaAs})_n/(\text{AlAs})_n$  SL's with  $n = 3-15$ , where we plotted transition energies determined from the PR (open and solid circles) and PL (crosses). It should be mentioned that the open and solid circles are direct (referred to as  $\Gamma$ ) and pseudodirect (referred to as  $X_z$ ) transition energies, respectively. The

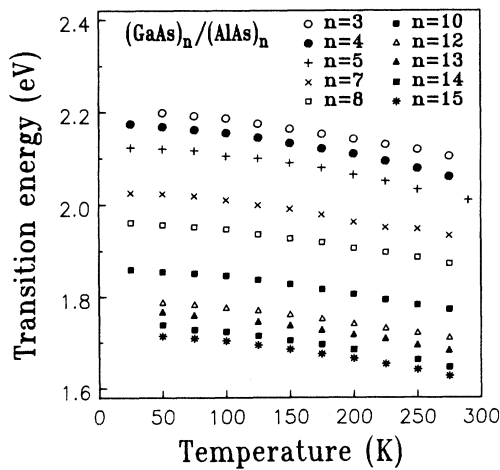


FIG. 5. The lowest allowed direct transition energy obtained by PR measurement are plotted as a function of temperature in the  $(\text{GaAs})_n/(\text{AlAs})_n$  SL's with  $n = 3, 4, 5, 7, 8, 10, 12, 13, 14, 15$  from the top to the bottom.

weak PR structures at the lower-energy side are not observed in all the samples investigated. Since the weak structure arises from the zone-folded  $X_z$ -like state, the optical transition depends strongly on the superlattice

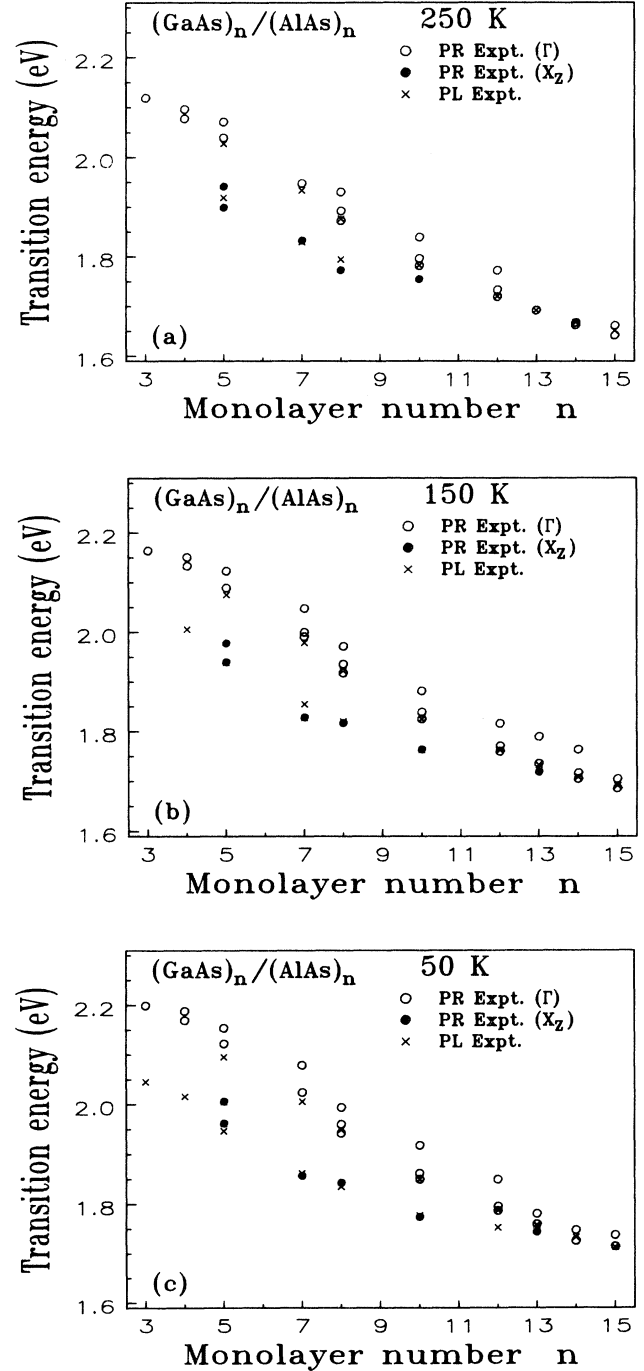


FIG. 6. Monolayer number dependence of the transition energies of the  $(\text{GaAs})_n/(\text{AlAs})_n$  SL's obtained from the present PR and PL measurements (a) at 250 K, (b) at 150 K, and (c) 50 K, where the open and solid circles represent the allowed direct and pseudodirect transition energies obtained by the PR measurements, respectively, and the crosses indicate the PL peak energies.

periods and thus the weak structure is affected by a fluctuation of the superlattice periods, resulting in missing a weak structure in some of the samples with small  $n$ . We find in Fig. 6 that the PR transition energies and PL peak energies decrease monotonically with increasing the number of layers  $n$ , and the pseudodirect PR transition and the lowest PL peak energies are lower than the direct PR transition energies for  $n < 14$  at 50 and 150 K, and for  $n < 12$  at 250 K. These results indicate an existence of a crossover of the direct-pseudodirect transitions in the  $(\text{GaAs})_n/(\text{AlAs})_n$  SL's. The direct-pseudodirect crossover depends on temperature, occurring at larger  $n$  as the temperature is decreased. One of the most probable possibilities for this temperature dependence may be the difference in the temperature dependence of the energy gaps of GaAs and AlAs, where the temperature dependence of the indirect gap in AlAs is slightly smaller than the direct gap of GaAs.

In our previous papers,<sup>27</sup> we reported that the experimental data of the PR and PL are well explained by the energy-band structures calculated by the  $sp^3s^*$  tight-binding method, where the direct-indirect crossover occurs at  $m = 7$  for  $(\text{GaAs})_m/(\text{AlAs})_5$  SL's. As stated in Sec. I of this paper and our previous paper<sup>28</sup> the weak structure was observed only in  $(\text{GaAs})_5/(\text{AlAs})_5$  SL, and therefore we ascribed the lower-energy peak of the PL to the indirect transition. The calculated results were found to be in reasonable agreement with the experimental results. As discussed in Sec. I, Lu and Sham<sup>30</sup> pointed out that the conduction band at the  $X$  point of bulk GaAs and AlAs is not well reproduced by the tight-binding calculations reported so far, and that the  $X_z$ -like state reflects the effective masses at the  $X$  point of AlAs. Lu and Sham<sup>30</sup> proposed a method to take into account the effective masses at the  $X$  point of AlAs in the second-nearest-neighbor  $sp^3$  tight-binding theory and showed that the lowest-energy transitions in our experimental data of  $(\text{GaAs})_m/(\text{AlAs})_5$  SL's with  $m \leq 7$  arise from the pseudodirect gap. Xia and Chang also have investigated the band structures of GaAs/AlAs SL's using this method<sup>31</sup> and obtained the same conclusion. Considering the results we adopt the method proposed by Lu and Sham in the present calculations and compare the calculated results with the present observations. We use the tight-binding parameters obtained by Lu and Sham.<sup>30</sup> These parameters reproduce the band edges and the associated effective masses for both GaAs and AlAs bulks. The valence-band offset is chosen to be 0.55 eV. We choose the mean values between the GaAs and AlAs bulks values for the tight-binding parameters affected by the interface in this calculation, since the band energies of  $(\text{GaAs})_n/(\text{AlAs})_m$  SL's with  $n$  or  $m$  less than 3 are not sensitive to these parameters.<sup>30</sup> The calculated results for the very-short-period SL's may be unreliable because of the lack of self-consistency of the interface parameters.

In Fig. 7 we plotted the lowest direct (solid curve), pseudodirect (dashed curve), and indirect (dot-dashed curve) transition energies obtained by the tight-binding calculations as a function of the monolayer number  $n$ ,

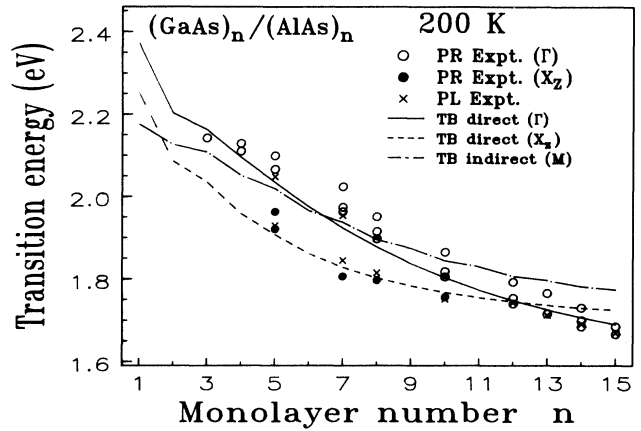


FIG. 7. Monolayer number dependence of the transition energies of the  $(\text{GaAs})_n/(\text{AlAs})_n$  SL's calculated by the second-nearest-neighbor  $sp^3$  tight-binding method, where the solid, dashed, and dot-dashed curves represent the lowest allowed direct, the lowest pseudodirect, and the lowest indirect (associated with the  $X_{xy}$ -like conduction state at  $M$  point) transition energies, respectively. The allowed direct and pseudodirect transition energies obtained from the PR measurements at 200 K are also shown by open and solid circles, respectively, and the PL peak energies at 200 K are shown by crosses. Calculated results were obtained by using the parameters reported by Lu and Sham (Ref. 30).

where we plotted transition energies determined from the PR (open and solid circles) and PL (crosses) at 200 K. The indirect gap energies plotted in Fig. 7 are the transition energies between the conduction-band minima at the  $M$  point (the  $X_{xy}$ -like states) and the valence-band top at the  $\Gamma$  point. The present calculations show that the lowest-energy transition is pseudodirect below  $n = 12$  and allowed direct above  $n = 12$ . This feature is in a good agreement with the present observation at 200 K, as shown in Fig. 7, where we find that in the range  $n$  less than 12, the transition energies determined from the main PR signals (open circles) agree with the allowed direct transition energies (solid curve), and those from the weak PR signals (solid circles) agree with the pseudodirect transition energies (dashed curve).

We find in Fig. 7 that the  $X_z$ -like state lies below the  $X_{xy}$ -like state (the  $M$  point, dot-dashed curve) for  $n > 1$ . This ordering of the  $X$ -like bands depends strongly on the anisotropy of the effective masses of the  $X$  valley of AlAs bulk.<sup>30</sup> Therefore, in the empirical band calculations of the SL's the fitting of the effective masses of bulks is important in addition to that of the band gaps. We find in Fig. 7 that the lowest conduction bands are  $X_{xy}$ -like for  $n = 1$ . Recently Ge *et al.* investigated the energy bands of very-short-period  $(\text{GaAs})_n/(\text{AlAs})_n$  SL's with  $n \leq 4$  by PL, and showed that the lowest conduction bands are  $X_{xy}$ -like for  $n \leq 3$  and  $X_z$ -like for  $n = 4$ .<sup>42</sup> The agreement is not good between their experiments and the present calculations. This could be

due to layer thickness fluctuations of the samples or the tight-binding parameters affected by the interface. In order to resolve such a discrepancy we have to check the effect of the layer thickness fluctuations of the samples on the band structures.<sup>28</sup> In addition we have to investigate how to determine the tight-binding parameters affected by the interface, because the ordering of the conduction bands for small  $n$  is strongly dependent on the parameters.

The results of the present work are summarized as follows. We carried out PR and PL measurements in  $(\text{GaAs})_n/(\text{AlAs})_n$  SL's with  $n = 3-15$  at the temperature range from 25 to 275 K in order to investigate the optical properties, placing our main interest in the zone-folding effect. We observed a weak structure in PR spectra below the main structure in  $(\text{GaAs})_n/(\text{AlAs})_n$  SL's with  $n$  less than about 12. The weak structure was ascribed to the pseudodirect transition between the folded  $X_z$ -like conduction state and the valence-band top. The main structure is interpreted in terms of the allowed direct transition between the  $\Gamma$ -like conduction state and the valence-band top. The temperature dependence of the

PL intensity ratio between the allowed direct and pseudodirect transitions has revealed that the probability of the pseudodirect transition is smaller by 3 or 4 orders of magnitude than that of the allowed direct transition. Our observations show that the direct-pseudodirect crossover in  $(\text{GaAs})_n/(\text{AlAs})_n$  SL's occurs for  $n = 14$  at 50 and 150 K, and for  $n = 12$  at 250 K, and thus the direct-pseudodirect crossover depends on temperature. Our observations are supported by the energy-band calculations based on the empirical  $sp^3$  tight-binding model including the second-nearest-neighbor interactions, where the direct-pseudodirect crossover is expected to occur for  $n = 12$  and the lowest conduction states are  $X_{xy}$ -like for  $n = 1$ .

#### ACKNOWLEDGMENT

This work was supported in part by a Grant-in-Aid for Scientific Research on Priority Area "Electron Wave Interference Effects in Mesoscopic Structures" from the Ministry of Education, Science and Culture.

- 
- <sup>1</sup>E. Finkman, M. D. Sturge, and M. C. Tamargo, *Appl. Phys. Lett.* **49**, 1299 (1986).  
<sup>2</sup>D. S. Jiang, K. Kelting, H. J. Queisser, and K. Ploog, *J. Appl. Phys.* **63**, 845 (1988).  
<sup>3</sup>M. Recio, J. L. Castano, and F. Briones, *Jpn. J. Appl. Phys.* **27**, 1204 (1988).  
<sup>4</sup>K. J. Moore, P. Dawson, and C. T. Foxon, *Phys. Rev. B* **38**, 3368 (1988).  
<sup>5</sup>K. J. Moore, G. Duggan, P. Dawson, and C. T. Foxon, *Phys. Rev. B* **38**, 5535 (1988).  
<sup>6</sup>H. Kato, Y. Okada, M. Nakayama, and Y. Watanabe, *Solid State Commun.* **70**, 535 (1989).  
<sup>7</sup>M. Nakayama, I. Tanaka, I. Kimura, and H. Nishimura, *Jpn. J. Appl. Phys.* **29**, 41 (1990).  
<sup>8</sup>J. N. Schulman and T. C. McGill, *Phys. Rev. B* **19**, 6341 (1979).  
<sup>9</sup>K. K. Mon, *Solid State Commun.* **41**, 699 (1982).  
<sup>10</sup>H. Rucker, M. Hanke, F. Bechstedt, and R. Enderlein, *Superlatt. Microstruct.* **2**, 477 (1986).  
<sup>11</sup>L. Brey and C. Tejedor, *Phys. Rev. B* **35**, 9112 (1987).  
<sup>12</sup>E. Yamaguchi, *J. Phys. Soc. Jpn.* **56**, 2835 (1987).  
<sup>13</sup>S. Nara, *Jpn. J. Appl. Phys.* **26**, 1713 (1987).  
<sup>14</sup>S. Nara, *Jpn. J. Appl. Phys.* **26**, 690 (1987).  
<sup>15</sup>J. Ihm, *Appl. Phys. Lett.* **50**, 1068 (1987).  
<sup>16</sup>J. Sanchez-Dehesa and C. Tejedor, *Phys. Rev. B* **26**, 5824 (1982).  
<sup>17</sup>D. Z.-Y. Ting and Y.-C. Chang, *Phys. Rev. B* **36**, 4359 (1987).  
<sup>18</sup>E. Caruthers and P. J. Lin-Chung, *Phys. Rev. B* **17**, 2705 (1978).  
<sup>19</sup>W. Andreoni and R. Car, *Phys. Rev. B* **21**, 3334 (1980).  
<sup>20</sup>M. A. Gell, D. Ninno, M. Jaros, and D. C. Herbert, *Phys. Rev. B* **34**, 2416 (1986).  
<sup>21</sup>J. B. Xia, *Phys. Rev. B* **38**, 8358 (1988).  
<sup>22</sup>T. Nakayama and H. Kamimura, *J. Phys. Soc. Jpn.* **54**, 4726 (1985).  
<sup>23</sup>D. M. Bylander and L. Kleinman, *Phys. Rev. B* **36**, 3229 (1987).  
<sup>24</sup>S.-H. Wei and A. Zunger, *J. Appl. Phys.* **63**, 5795 (1988).  
<sup>25</sup>Y. Hatsugai and T. Fujiwara, *Phys. Rev. B* **37**, 1280 (1988).  
<sup>26</sup>S. Massidda, B. I. Min, and A. J. Freeman, *Phys. Rev. B* **38**, 1970 (1988).  
<sup>27</sup>T. Nakazawa, H. Fujimoto, K. Imanishi, K. Taniguchi, C. Hamaguchi, S. Hiyamizu, and S. Sasa, *J. Phys. Soc. Jpn.* **58**, 2192 (1989).  
<sup>28</sup>H. Fujimoto, C. Hamaguchi, T. Nakazawa, K. Taniguchi, K. Imanishi, H. Kato, and Y. Watanabe, *Phys. Rev. B* **41**, 7593 (1990).  
<sup>29</sup>P. Vogl, H. P. Hjalmarson and J. D. Dow, *J. Phys. Chem. Solids* **44**, 365 (1983).  
<sup>30</sup>Y. T. Lu and L. J. Sham, *Phys. Rev. B* **40**, 5567 (1989).  
<sup>31</sup>J. B. Xia and Y. C. Chang, *Phys. Rev. B* **42**, 1781 (1990).  
<sup>32</sup>C. Hamaguchi, T. Nakazawa, T. Matsuoka, T. Ohya, K. Taniguchi, H. Fujimoto, K. Imanishi, H. Kato, and Y. Watanabe, in *SPIE International Conference on Modulation Spectroscopy*, edited by F. H. Pollak, M. Cardona, and D. E. Aspnes (SPIE, Bellingham, 1990), p. 280.  
<sup>33</sup>C. Hamaguchi, T. Nakazawa, T. Matsuoka, T. Ohya, K. Taniguchi, H. Fujimoto, K. Imanishi, H. Kato, and Y. Watanabe, in *20th International Conference on the Physics of Semiconductors*, Tessaaloniki, Greece, 1990, edited by E. M. Anastassakis and J. D. Joannopoulos (World Scientific, Singapore, 1990), p. 1033.  
<sup>34</sup>N. Sano, H. Kato, M. Nakayama, S. Chika, and H. Terauchi, *Jpn. J. Appl. Phys.* **23**, L640 (1984).  
<sup>35</sup>H. Terauchi, Y. Noda, K. Kamigaki, S. Matsunaka, M. Nakayama, H. Kato, N. Sano, and Y. Yamada, *J. Phys. Soc. Jpn.* **57**, 2416 (1988).  
<sup>36</sup>T. Nakazawa, T. Matsuoka, T. Ohya, K. Taniguchi, C. Hamaguchi, H. Kato, and Y. Watanabe, in *SPIE Inter-*

- national Conference on Modulation Spectroscopy* (Ref. 32), p. 244.
- <sup>37</sup>J. L. Shay, *Phys. Rev. B* **2**, 803 (1970).
- <sup>38</sup>O. J. Glembocki, B. V. Shanabrook, N. Bottka, W. T. Beard, and J. Comas, *Appl. Phys. Lett.* **46**, 970 (1985).
- <sup>39</sup>D. E. Aspnes and J. E. Rowe, *Phys. Rev. B* **5**, 4022 (1972).
- <sup>39</sup>D. E. Aspnes and J. E. Rowe, *Phys. Rev. B* **5**, 4022 (1972).
- <sup>40</sup>D. E. Aspnes, *Surf. Sci.* **37**, 418 (1973).
- <sup>41</sup>H. H. Rosenbrock, *Comput. J.* **3**, 175 (1960).
- <sup>42</sup>W. Ge, M. D. Sturge, W. D. Schmidt, L. N. Pfeiffer, and K. W. West, *Appl. Phys. Lett.* **57**, 55 (1990).